



Article

Enhancing Wind Erosion Assessment of Metal Structures on Dry and Degraded Lands through Machine Learning

Marta Terrados-Cristos ^{*}, Francisco Ortega-Fernández, Marina Díaz-Piloñeta, Vicente Rodríguez Montequín 
and José Valeriano Álvarez Cabal

Project Engineering Department, University of Oviedo, 33004 Oviedo, Spain

* Correspondence: marta.terrados@api.uniovi.es

Abstract: With the increasing construction activities in dry or degraded lands affected by wind-driven particle action, the deterioration of metal structures in such environments becomes a pressing concern. In the design and maintenance of outdoor metal structures, the emphasis has mainly been on preventing corrosion, while giving less consideration to abrasion. However, the importance of abrasion, which is closely linked to the terrain, should not be underestimated. It holds significance in two key aspects: supporting the attainment of sustainable development goals and assisting in soil planning. This study aims to address this issue by developing a predictive model that assesses potential material loss in these terrains, utilizing a combination of the literature case studies and experimental data. The methodology involves a comprehensive literature analysis, data collection from direct impact tests, and the implementation of a machine learning algorithm using multivariate adaptive regression splines (MARS) as the predictive model. The experimental data are then validated and cross-verified, resulting in an accuracy rate of 98% with a relative error below 15%. This achievement serves two primary objectives: providing valuable insights for anticipating material loss in new structure designs based on prospective soil conditions and enabling effective maintenance of existing structures, ultimately promoting resilience and sustainability.

Keywords: wind erosion; degraded land; metal structures; abrasion; machine learning



Citation: Terrados-Cristos, M.; Ortega-Fernández, F.; Díaz-Piloñeta, M.; Montequín, V.R.; Cabal, J.V.Á. Enhancing Wind Erosion Assessment of Metal Structures on Dry and Degraded Lands through Machine Learning. *Land* **2023**, *12*, 1503. <https://doi.org/10.3390/land12081503>

Academic Editor: Chuanrong Zhang

Received: 16 June 2023

Revised: 22 July 2023

Accepted: 26 July 2023

Published: 28 July 2023



Copyright: © 2023 by the authors. Licensee MDPI, Basel, Switzerland. This article is an open access article distributed under the terms and conditions of the Creative Commons Attribution (CC BY) license (<https://creativecommons.org/licenses/by/4.0/>).

1. Introduction

Wind erosion is a natural process that involves removal, transport and deposition of coarse and fine particles, primarily sand, by the wind [1]. Differences in atmospheric pressure generate air movements capable of eroding surface materials (also known as abrasion) when velocities reach sufficient levels [2]. The scientific community has increasingly recognized the significance of wind erosion due to its impact on soil health, agricultural production, climate and structures resilience [3]. Efforts have been devoted to simulating and predicting wind-driven effects, including soil erosion, to control land degradation and implement appropriate agricultural management practices [4]. Various methods, ranging from empirical equations for average soil erosion [5,6] to advanced models predicting crop yields and conservation of natural resources [7–9], have been developed.

However, wind erosion is gaining increasing relevance in other fields that have not been extensively studied. The durability of metal structures is greatly influenced by damage caused by wind erosion, particularly in degraded areas where wind-driven particle movement is more intense [10]. While the degradation of metal structures in outdoor conditions, both chemically and physically, is directly influenced by their geographical location [11], the attention has predominantly been on studying corrosion [12–14], with less emphasis on terrain-related abrasion, which holds relevance for achieving sustainable development goals and effective land planning.

Identifying and determining suitable soils for construction would facilitate their classification, allowing for redirection to alternative uses or assigning specific wear values,

aligning with the objectives of sustainable development, and minimizing material wastage. This process results in significant economic, social, and environmental losses, affecting various metal constructions.

Windblown sand transport is characterized by three types of movement based on grain diameter (d): suspension ($d < 0.07$ mm); saltation ($0.07 < d < 0.5$ mm); and creep ($d > 0.5$ mm) [15] (Figure 1). Among these, saltation plays a crucial role in the total mass of sand transported, driven by wind shear forces on the land surface that lead to the rebound of sand particles and horizontal sand mass flow in the downwind direction [16,17].

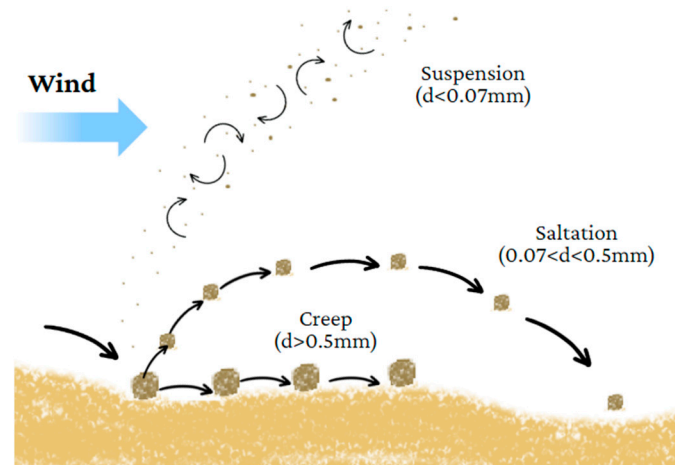


Figure 1. Windblown sand transport modes.

Although wind erosion can occur in all climates, it is more prevalent in semi-arid and arid environments characterized by extensive land degradation or dry conditions [18]. As a result, metal structures were historically not exposed to this problem. However, the proliferation of constructions in these areas, including new cities [19] and the development of renewable energy projects [20,21], has brought wind erosion into focus. Approximately one-fifteenth of the Earth's surface is susceptible to significant sand blowing [16] and the expansion of wind erosion-prone areas is expected due to climate change [22].

Factors influencing the movement of sand and hazardous particles by wind include specific particle size distribution, extensive plain lands without vegetation or wind barriers, high wind speeds combined with low relative humidity and elevated concentrations of total suspended particulate matter [23]. In contrast, as height increases, the negative impact of the process becomes less severe due to its inherent characteristics, as higher altitudes result in fewer particles reaching the area [24,25]. The parameters that influence erosion can be categorized into three main groups.

1. Impact conditions, which include the velocity and angle of impact;
2. Characteristics of the eroding particle, such as its size, shape, and other parameters;
3. Properties of the material being eroded, including its ductility, hardness, density, and other relevant factors.

Understanding how land conditions affect infrastructure in the long term is crucial for the design and maintenance of both new and historic buildings. The maintenance of structures in aggressive environments, such as the north-west coast of Egypt exposed to sandstorms, presents significant challenges [26]. Wind erosion implications for high-speed lines in Saudi Arabia are also garnering attention [27]. Researchers at the Inner Mongolia University of Technology have studied the impact of wind erosion on steel structure coatings in central and western regions of Mongolia affected by sandstorms [28,29]. However, the design, analysis, and evaluation of wind erosion processes are still in the early stages of study.

Common responses to wind erosion include increasing protection and coating of materials, which is prevalent in the wind and aeronautics industry, with research exploring

multilayer coatings and alloys [30,31]. Prior knowledge during the design or engineering phase is essential for sustainability as it facilitates calculations that help to mitigate the economic and environmental implications of excessive material waste [32]. Other studies have focused on soil treatment solutions, such as protective barriers [33] or surface treatments [34–36], but implementing these solutions on larger surfaces is challenging. The current approach to studying wind erosion often relies on localized and case-specific investigations, compounded by a lack of standardized terminology in the literature. These factors pose challenges in unifying the research efforts and effectively addressing the issue. Therefore, it is imperative to establish methods for determining and predicting the extent of wind erosion-induced abrasion on structures to enable the implementation of appropriate preventive measures.

The objective of this study is to develop a predictive machine learning model capable of determining the erosion rate experienced by metal structures based on their geographical location. By integrating data from various sources, including existing studies and experimental data, the model aims to provide insights into potential degradation associated with the surrounding land. These insights enable to design environmentally conscious structures, optimize material usage, and extend the lifespan of metal structures through careful maintenance planning and preventive measures.

This paper presents a detailed description of the methodology employed, starting with the creation of a robust database serving as the foundation for training the predictive models. The database comprises information sourced from existing studies in the literature. Given the limited literature data available, a specific and comprehensive dataset was generated, incorporating a wider range of materials and measurable variables obtained through direct impact tests conducted in a laboratory setting. Subsequently, the modelling techniques and evaluation methods utilized throughout this study are elucidated. Finally, the results are thoroughly analysed, and the conclusions drawn from this research are presented.

2. Materials and Methods

The methodology employed in this study is outlined in Figure 2 and encompasses three key phases. The initial phase involved the creation of a database, which serves as the key point for the application of predictive algorithms that facilitate the estimation of erosion rates for specific metals under different conditions and types of terrain. Subsequently, in the second phase, the model was developed based on the analysis of the compiled data. Finally, in the third phase, the model's efficacy was evaluated through validation procedures, and the obtained results were assessed.

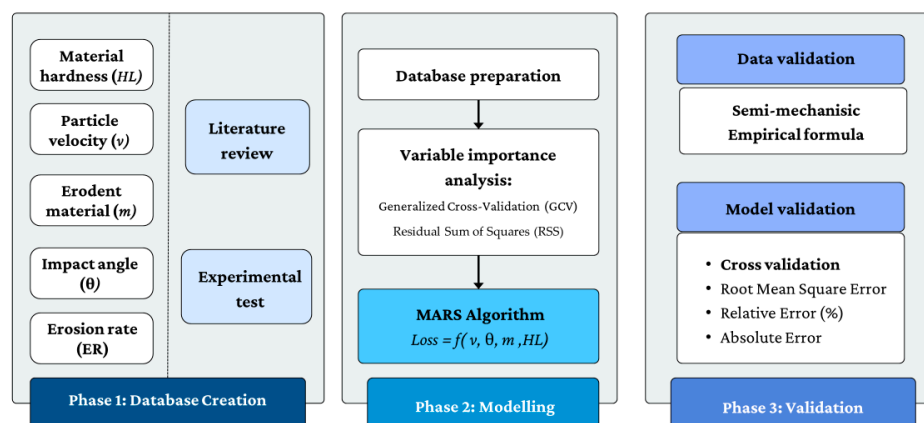


Figure 2. Overall process followed.

2.1. Phase 1: Database Creation

For this first phase, two main sources of data were used: external data derived from international literature, and internal data acquired from experimental laboratory tests. The first source involved assembling the cases and analysis of the relevant information in the

literature related to the study topic. Additionally, several laboratory tests were carried out in order to expand the information with our own experimental data.

2.1.1. Literature Review

Erosion is a phenomenon influenced by multiple factors, including the properties of both the material being eroded and the material causing the erosion, as well as the conditions under which the phenomenon occurs. Table 1 summarises the most significant variables considered in the literature.

Table 1. Most significant variables of the direct impact test.

Process Parameters	Eroded Material Parameters
Impact angle [37]	Hardness [38]
Particle diameter of impacting particles [39]	Fracture toughness [38]
Impact velocity [40]	Elastic modulus [37]

However, to attempt a macroscopic approach and ensure that the model is truly useful and applicable to any case study, the variables that form the model should be readily available or easily obtainable. Therefore, the variables collected were selected based on their availability and significance according to the literature.

1. Material hardness (*HL*): Studies agree that material hardness is a highly influential variable in calculating wind erosion [41];
2. Particle velocity (*v*): It is key point to determine the force with which particles impact the structure, as abrasion increases with higher particle velocities [41];
3. Amount of erodent material (*m*): The quantity of material impacting the structure directly influences the level of abrasion [41];
4. Impact angle (θ): Studies have shown that for ductile materials as metallic structures, the highest abrasion damage occurs at impact angles between 15 and 30 degrees and decreases towards 90 degrees [42];
5. Erosion rate (*ER*): The majority of scientific literature describes wind erosion using the erosion ratio which is usually measured as follows (1) [43,44]:

$$ER = \frac{\text{Mass of material lost due to erosion}}{\text{Mass of material eroded}} \quad (1)$$

Measuring the impact in this way, instead of using mass loss, has the advantage of allowing better comparison of erosion between different materials [45]. At this point, all experimental studies in the literature that aim to characterize the effect of different parameters on erosion and erosion resistance of various materials were collected. These studies typically involve conducting tests with sand or other particles and measuring the impact [42,46].

The database consists of 778 data points. The dataset, comprising data from different laboratory tests, undergoes thorough pre-processing to handle missing values, outliers, and inconsistencies. Standardisation of measurement units is applied to facilitate meaningful comparisons, while min-max scaling rescales the variables for analysis. Categorical data are appropriately encoded, and the normalized data from various sources are integrated into a unified dataset stored as relational data in a CSV (comma-separated values) format.

2.1.2. Experimental Test

Experimental data were obtained by conducting various laboratory tests. The analysed and collected variables were the same as those identified as relevant in the literature review. The procedure for obtaining each of these experimental data is specified below.

Material Hardness (*HL*)

Hardness tests were performed on plates made of different materials using the Leeb hardness test. The Leeb hardness (*HL*) [47] relates the rebound velocity to the impact velocity of a spherical device, with a diameter of 3 mm or 5 mm (2).

$$HL = \frac{\text{rebound velocity}}{\text{impact velocity}} \times 1000 \quad (2)$$

The tests were performed according to the following standards: ASTM A956/A956m–17a, Standard Test Method for Leeb Hardness Testing of Steel Products and ISO 16859-1/2/3:2015, and Metallic materials–Leeb hardness test [48,49].

Particle Velocity (*v*)

Velocity can be adjusted based on factors such as the pressure of the compressor, atmospheric pressure, and the diameter of the nozzle. By measuring the air velocity, we can estimate the particle velocity and determine its range of values. According to studies in the literature, the relationship with the velocity of the carrier fluid itself is estimated to be less than one-third [42].

Amount of Erodent Material (*m*)

The material impacting the structure can be estimated based on the concentration of erodent material in the air (expressed in micrograms per cubic meter) (m_a), multiplied by the wind velocity (in meters per second) (v_w); the duration of impact per year (in hours) (d); and the surface area (in square meters) (s) (3). At a laboratory level, the amount of sand is determined via weighing.

$$m = m_a * v_w * d * s \quad (3)$$

Impact angle (θ)

The impact angle (θ) can be determined by comparing the orientation of the structure with the dominant wind direction. At a laboratory level, the impact angle can be set by sample's colocation.

Erosion Rate (*ER*)

Erosion rate was determined by conducting direct impact tests according to the ASTM G76-2013 standard [50]. A total of 216 tests were conducted, involving 12 different types of materials, including bare steel, stainless steel, galvanized steel, aluminium, and tinplate. Each material underwent 3 repetitions of the test. The tests were performed using 3 batches of 300 g of sand, resulting in a total of 900 g of eroding particles. Two different sizes of sand were used (150 and 300 μm).

All these tests were carried out in a sandblasting cabin (CHC60, PA, Spain) equipped with a sandblasting gun operated with ceramic nozzles. The required airflow rate of 340 L/min was achieved using a compressor (METALWORKS 458804090, PA, Spain). Figure 3 shows an outline of the testing procedure. To separate the sand into different particle sizes, a sieve shaker (CISA BA200N, PA, Spain) was employed.

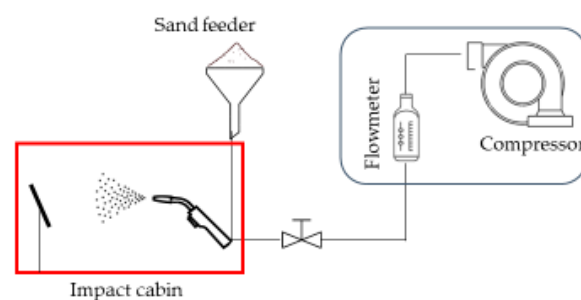


Figure 3. Schematic representation of laboratory tests performed.

The plates were weighed before and after each sand batch using Laboratory Precision Balance (Raswag AS 310 R2 PLUS, PA, Spain) to determine the mass loss. By comparing the final weight with the initial weight, the mass loss caused by the impact was determined, providing valuable information about the energy absorption capacity of the samples and the erosion ratio (*ER*).

2.2. Phase 2: Modelling

Once all the data are collected, complementing the information from the literature with experimental test, the modelling stage began. The collected data from both sources underwent a thorough cleaning and pre-processing process to ensure data quality and consistency. An exploratory analysis was conducted to understand the data structure and identify patterns. Relevant variables were selected for predictive models. Two methods are used to determine the importance of each variable in the model: generalized cross-validation (GCV) and residual sum of squares (RSS).

- Generalized cross-validation (GCV): It involves fitting the model with all variables, calculating GCV scores by temporarily excluding each variable, and ranking them based on their scores. Variables with higher GCV scores are considered more important;
- Residual sum of squares (RSS): It calculates the sum of the squared differences between the observed values and the predicted values obtained by the model. The RSS represents the overall amount of unexplained variation in the data. A lower RSS indicates a better fit of the model to the data.

The database was then prepared for model construction by partitioning the data and handling missing values. These steps ensured the integrity of the data and facilitated the construction of accurate predictive models.

The modelling stage is carried out using the MARS algorithm (multivariate adaptive regression splines). This algorithm is an effective tool for constructing accurate and robust predictive models from complex datasets. MARS algorithm enables the identification of nonlinear and nonparametric relationships among variables, which is particularly useful in the study of direct impact where relationships can be highly nonlinear. This machine learning technique combines linear regression with non-linear functions called splines. It begins by constructing an initial linear model and then adds splines to capture non-linear relationships in the data. It uses an iterative approach to improve the fit and selects the most relevant variables [51]. Ultimately, a flexible model is obtained that combines both linear and non-linear terms to predict a continuous response variable [52].

The MARS algorithm is capable of predicting the amount of material that can be lost due to abrasion, as shown in Equation (4) in the following form:

$$Loss (g) = f(v, \theta, m, HL) \quad (4)$$

where

- v : Particle velocity (m/s);
- θ : Impact angle ($^{\circ}$);
- m : Mass of sand (g);
- HL : Material hardness.

2.3. Phase 3: Validation

Validating the obtained results is crucial to ensure the reliability and generalizability of the developed models. In this methodology, two validation phases are conducted: data validation and model validation.

2.3.1. Data Validation

To validate the obtained results, it is proposed to employ an empirical semi-mechanistic erosion equation [37]. This formula is based on theoretical principles and physical laws

related to direct impact. By comparing the data with the values calculated, the consistency and validity of the obtained results can be evaluated.

The erosion damage is caused by two mechanisms: cutting (ER_C) (5) and deformation (ER_D) (6). Therefore, the total erosion damage is given by the sum of both terms.

$$ER_C = \begin{cases} C_1 F_s \frac{U^{2.41} \sin(\theta) [2 K \cos(\theta) - \sin(\theta)]}{2K^2} & \theta < \tan^{-1}(K) \\ C_1 F_s \frac{U^{2.41} \cos^2(\theta)}{2} & \theta > \tan^{-1}(K) \end{cases} \quad (5)$$

$$ER_D = C_2 F_s \frac{(U \sin(\theta) - U_{tsh})^2}{2} \quad (6)$$

where

- U_{tsh} is the threshold velocity below which deformation is negligible;
- F_s is the angularity factor of the particle, ranging from 0.25 for completely rounded particles to 1 for very angular particles. In this case, F_s was considered as 0.5;
- K is the ratio between the contact area in the x-direction and the contact area in the y-direction of the particle with the material. In most materials eroded by sand, it is 0, so is the ratio used in this study;
- C is the cutting constant, which depends on the hardness of the material. It has been shown to be proportional to the inverse square root of materials hardness [42];
- U is the initial velocity of the particle. According to experimental studies, the average relationship between particle velocity and gas velocity is 3.1739 [42];
- θ is the impact angle, considered perpendicular in this case.

2.3.2. Model Validation

Cross-validation is a widely used technique for evaluating the performance of predictive models. In this context, the dataset is divided into training (75%) and testing (25%) subsets. The model is trained using the training subset, and its performance is evaluated using the testing subset. This process is repeated several times (6 blocks), alternating the training and testing subsets, and an average performance measure is calculated to assess the model's generalization capability, based on the following.

- The root mean square error (RMSE) measures the average magnitude of the residuals (differences between predicted and actual values). A lower RMSE indicates a better fit between the model and the observed data;
- Relative error measures the percentage difference between the predicted and actual values, providing insight into the relative accuracy of the model's predictions;
- Absolute error represents the absolute difference between predicted and actual values, giving an indication of the magnitude of the prediction errors;
- Mean directly compares the values, indicating the overall bias of the model.

3. Results

The results are presented in detail throughout the different phases of the proposed methodology.

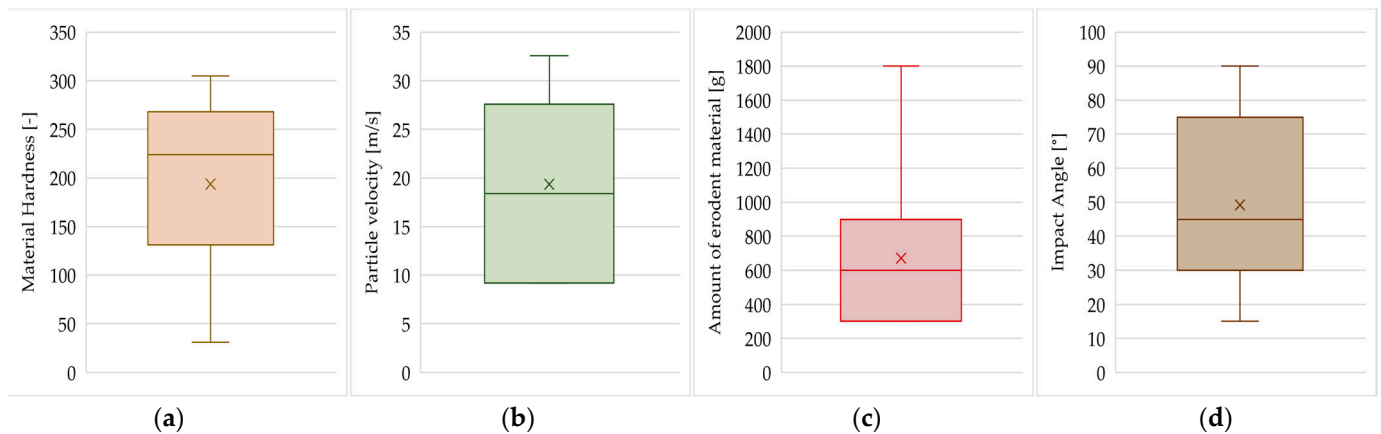
3.1. Phase 1: Database Creation

After an exhaustive study of the scientific literature and analysis of direct impact tests from research such as [46,53,54], the data and variables that align with the context of the object of this study are collected, analysed, identified, and added. A total of 778 initial data points were collected before eliminating and cleaning the database. The collected parameters and the range of values studied are summarised in the following Table 2.

Table 2. Values in the study variables: range, mean and standard deviation (Sd).

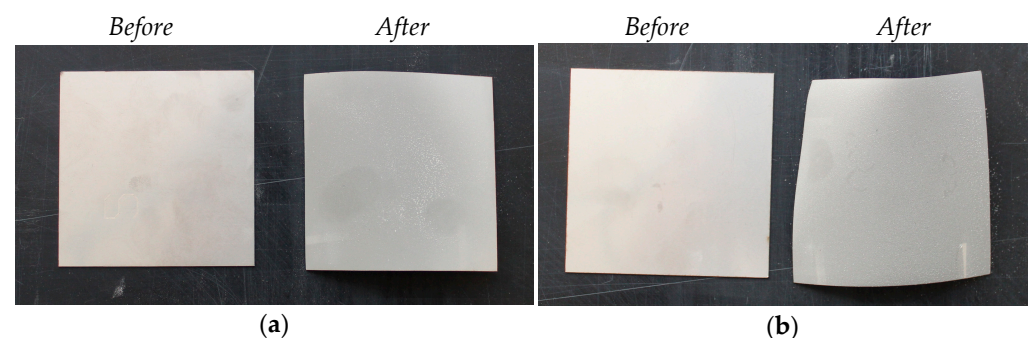
Material Hardness [-]			Particle Velocity [m/s]			Amount of Erodent Material [g]			Impact Angle [°]		
Range	Mean	Sd	Range	Mean	Sd	Range	Mean	Sd	Range	Mean	Sd
395–710	193.64	87.49	9.2–32.56	19.35	7.29	300–1800	670.65	343.25	15–90	49.22	25.71

The distribution of these variables is shown in the form of box plots in Figure 4.

**Figure 4.** Variable distribution: (a) material hardness, (b) particle velocity, (c) amount of erodent material, (d) impact angle.

On the other hand, the experimental tests were conducted under normal pressure and temperature conditions. The eroding material particles, in this case sand, had diameters of 150 μm and 300 μm and were propelled at a velocity ranging between 13 and 14 m/s.

Upon the completion of the impact tests, clear surface deformation was observed in the samples. Furthermore, evident surface changes were measured, indicating the influence on the structure and external appearance of the samples, suggesting the need for further detailed analysis. Some examples of the experimental test results are shown in Figure 5.

**Figure 5.** Metal samples before and after direct impingement tests. (a) Stainless steel, (b) galvanized steel.

It was observed that some plates, such as aluminium, showed mass gains of up to 0.05%. This phenomenon can be attributed not only to the absence of significant wear but also to the embedding of sand particles in the material. This phenomenon was also observed in tinplate samples. The remaining plates exhibited mass losses ranging from approximately 0.20% to 0.30%, except for galvanized steel, which showed losses of 0.99%.

The radial chart in Figure 6 displays the average values of each of the 12 materials under different test conditions. Mass loss after impact for the three defined amounts of sand, as well as the total mass loss, is shown in four different colours. In this following

chart, the axes extend outward from the centre and the magnitude of the mass loss is represented on each axis using dots or lines.

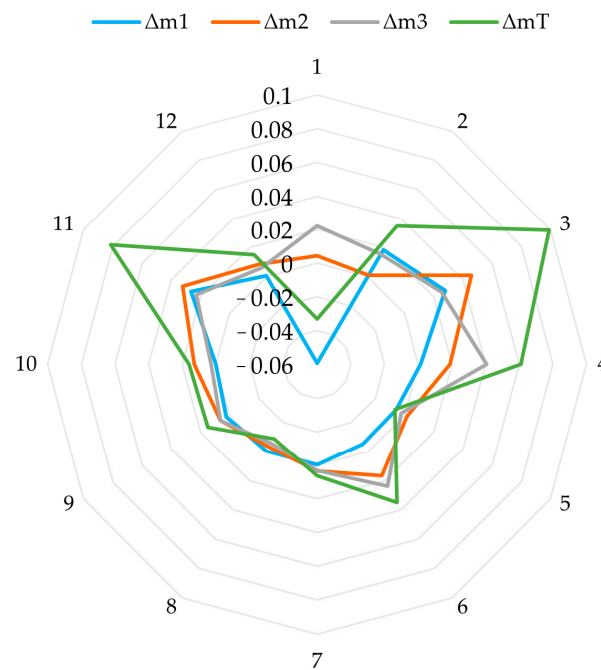


Figure 6. Representation of the average mass change in each study condition.

By comparing the mass losses among the different amounts of sand (300 g (Δm_1), 600 g (Δm_2) and 900 g (Δm_3)), patterns or trends can be identified. The chart shows that as the amount of sand increases, the mass loss also increases, except for materials where sand particles become embedded due to their low hardness. Additionally, the chart presents the total mass loss as a consolidated measure across all amounts of sand.

On the other hand, Figure 7 provides information about the distribution and variability of hardness values. It can be observed that the majority of values are within a close range, with a single outlier, corresponding to aluminium.

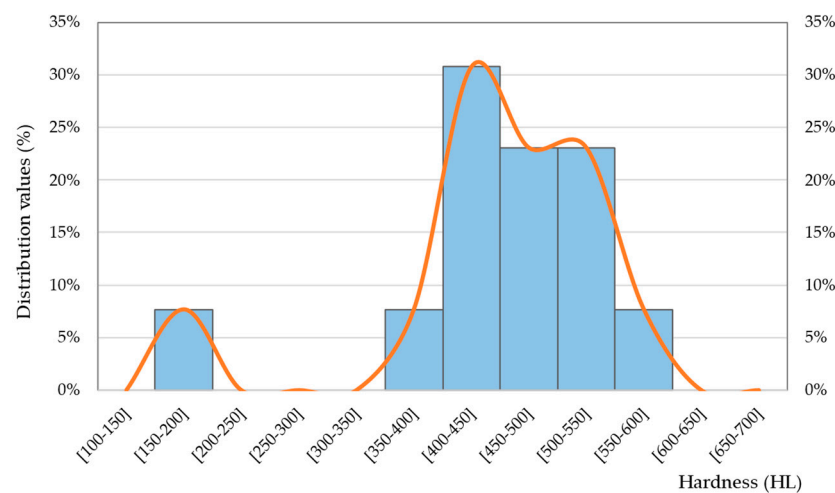


Figure 7. Representation of the hardness distribution of the tested materials.

The Pearson correlation coefficient obtained between mass change and hardness is 0.28, indicating a moderate positive correlation between hardness data and mass loss. The p -value of 0.361 suggests that this correlation is not statistically significant at a significance level of 0.05. It is important to note that other factors or variables not considered in

this analysis could have a more relevant influence on the results. Therefore, further comprehensive studies are recommended to better understand the nature and strength of the relationship between the variables in question.

3.2. Phase 2: Modelling

Once the database is prepared, the predictive algorithm is applied to create a model for predicting the material loss (mass loss) that a metal structure will experience under those conditions.

Two methods are used to determine the importance of each variable in the model: generalized cross-validation (GCV) and residual sum of squares (RSS). The most significant variables, in order, are shown in Table 3.

Table 3. Importance of each variable determined via GCV and RSS.

	GCV	RSS
Velocity	100	100
Impact Angle	76.2	76.2
Amount of Sand	62.9	62.9
Material Hardness	27	27.8

Velocity of impact is the most relevant factor according to both methods. Furthermore, the values obtained for each of the variables according to the two methods are similar and coherent with each other. Hence, these variables can be deemed as valid and integrated into the predictive model.

3.3. Phase 3: Validation

Figure 8 displays the results after validating the data obtained empirically through experimental trials and the data calculated using well-established equations in the scientific community. The dashed line represents the ideal situation for these values. Each set of experiments samples is represented by a unique colour. It can be observed that there are no significant deviations between the theoretical and practical values, and the differences are acceptable ($R^2 = 0.9207$). Therefore, these results can be considered valid and incorporated into the predictive model.

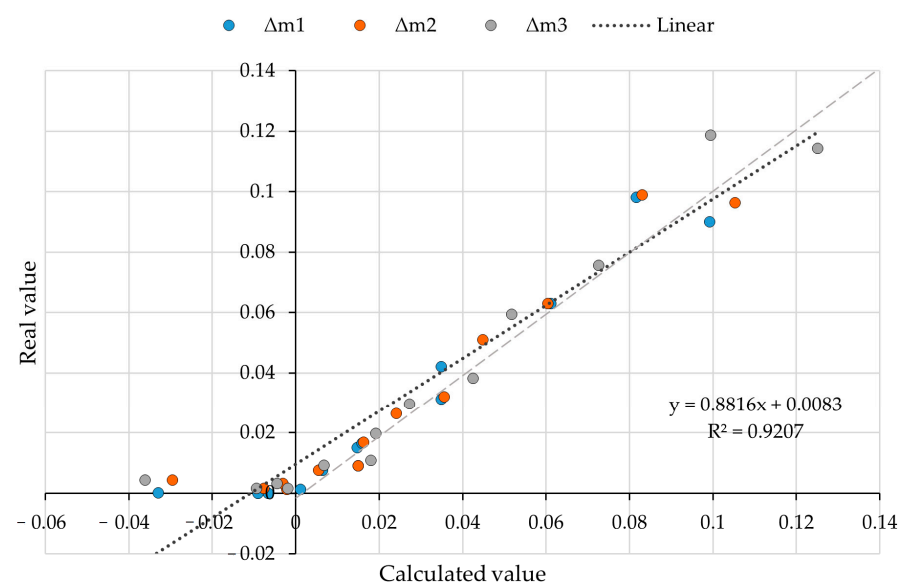


Figure 8. Comparison between experimentally and theoretically obtained results.

In Figure 9, the predicted values are represented on the vertical axis, while the actual values are shown on the horizontal axis.

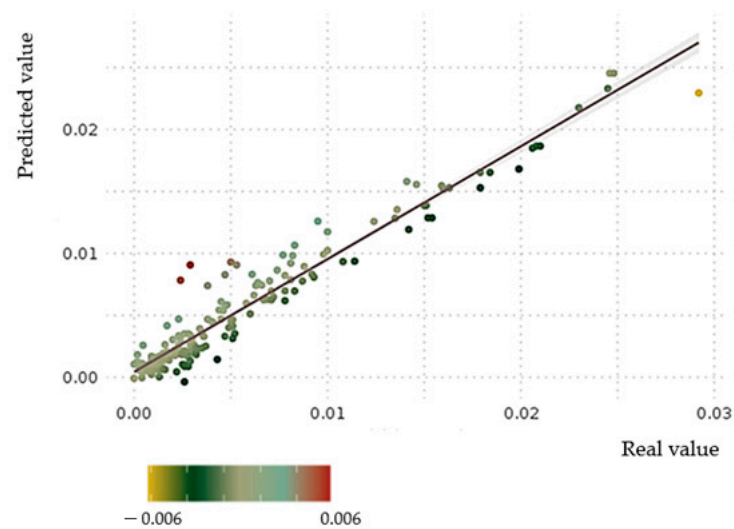


Figure 9. Abrasion model results.

Ideally, the points in this plot should be distributed along the diagonal line, indicating an exact correspondence between the model's predictions and the actual values. In this case, a high correlation is observed between the predicted and actual values, as most of the points are close to the diagonal line ($R^2 = 0.9083$). This demonstrates that the MARS model is capable of generating accurate estimations of mass loss based on the study parameters.

The proximity of the points to the diagonal line also suggests that the model generalizes well, meaning it can provide accurate predictions even for data not used during the model's training. This ability to generalize is essential to ensure the applicability and reliability of the model in practical situations.

The residuals represent the differences between the predicted and actual values of mass loss based on the study parameters. In a precise and reliable model, the residuals should be randomly distributed around zero and show no systematic trend.

In Figure 10, a homogeneous distribution of residuals around zero is observed, indicating that the MARS model can capture the variability in the data, adequately adjusting to the patterns of mass loss.

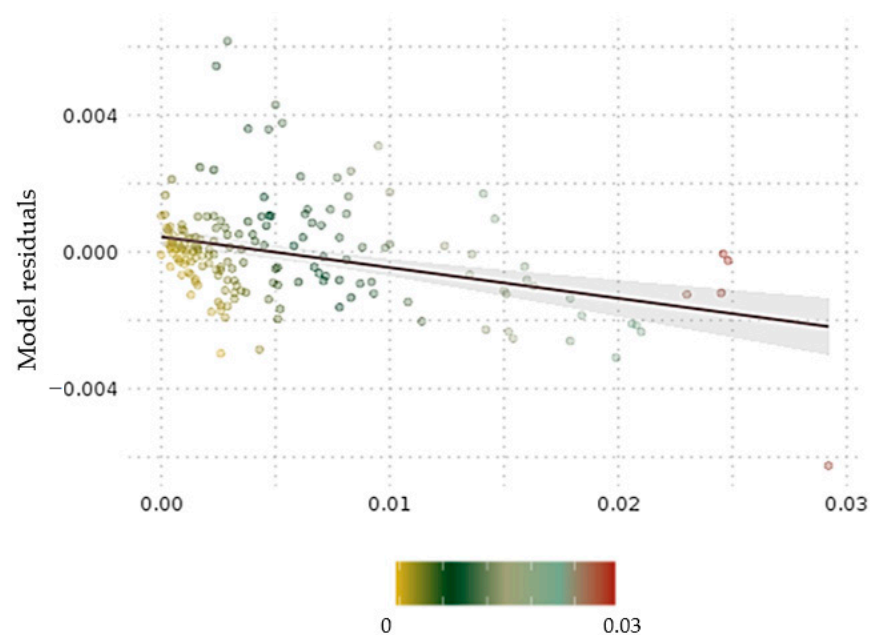


Figure 10. Residual plot of the MARS model.

The root mean square error (RMSE) used in this case to measure the differences between the predicted values of the model and the actual values has a value of 0.005587. Table 4 shows a comparison between the relative error, absolute error, the percentage predicted through the model, and an example of what it would be using the mean value.

Table 4. Relative error, absolute error, and mean error of the model.

Relative Error (%)	Absolute Error	Mean (%)	Model (%)
1	0.000292	1.12	25.7
5	0.00146	15.08	77.09
10	0.00292	38.55	94.41
14	0.004088	58.1	97.77
20	0.00584	85.47	98.88
25	0.0073	86.59	100
Inf	Inf	100	100

These results provide an assessment of the model's performance in predicting the abrasion values. The RMSE value indicates the average difference between the predicted and actual values, with lower values indicating better accuracy. The table presents the relative and absolute errors for different percentages, comparing the model's predictions to the mean value. It can be observed that the model's predictions have significantly lower errors compared to using the mean value, demonstrating its effectiveness in estimating the abrasion values. For a relative error of less than 15%, the model shows an efficiency of 98% accuracy.

4. Discussion

4.1. Interpretation of Results

The results of this study highlight the importance of considering the conditions and characteristics of the surrounding terrain when designing and maintaining outdoor metal structures on dry and degraded lands. This study emphasizes that wind erosion can lead to significant degradation of metal structures in such environments, a factor often overlooked during the design process. The developed predictive model incorporating data from various sources provides valuable insights into the potential material degradation and erosion experienced by these structures. The findings underscore the significance of including terrain-related parameters as essential factors in the design and maintenance practices for outdoor metal structures.

The compilation of a comprehensive database from the existing literature and the inclusion of experimental data from direct impingement tests on metal plates subjected to high-pressure air and sand impacts the study's findings. The experimental tests revealed mass losses ranging from 0.20% to 0.99% for different metal plates. It was interesting to observe that certain plates, such as aluminium and various types of tinplate, showed mass gains, likely due to minimal wear and the embedding of sand particles. These observations underscore the complexity of abrasion processes and highlight the need for a more nuanced understanding of material responses under different impact conditions.

4.2. Implications and Applications

The study's implications are significant for the construction industry and outdoor metal structure maintenance. By incorporating information about the land and drylands circumstances and environmental factors into the design process, engineers and designers can better anticipate and mitigate potential material loss and degradation. Understanding the impact of wind-driven particle action on metal structures will facilitate more informed decision-making in product development and material selection, ultimately leading to more durable and resilient structures.

The developed predictive model using the multivariate adaptive regression splines (MARS) algorithm holds great promise for practical applications. The model's accuracy in predicting material mass loss based on parameters such as hardness, impact angle, impact

velocity, and sand quantity makes it a valuable tool in assessing material performance and durability under different impact conditions. Designers and engineers can use this model to optimize the design of metal structures and select appropriate materials, considering the specific environmental conditions they will be exposed to. Moreover, the model's efficiency of 98% accuracy for a relative error of less than 15% indicates its reliability and suitability for real-world applications.

4.3. Limitations and Future Research

The present study offers valuable insights into the relationship between terrain conditions and material degradation, focusing on outdoor metal structures in a controlled environment. Although this study acknowledges certain limitations, it could be further enhanced to explore the significance of its findings in dryland regions, where the impact of environmental factors is more pronounced.

One aspect that could be clarified is how dryland conditions were specifically modelled in the lab. Understanding the methodology used to replicate these conditions would add depth to the study and provide insight into the relevance of the findings to real-world desert environments.

To enhance the study's applicability, future research should consider in situ challenges that may be encountered in actual deserts. Factors such as extreme temperature fluctuations, the presence of abrasive particles in winds, and limited water resources for structure maintenance can significantly affect material degradation in dryland areas.

Moreover, investigating the long-term performance of the predictive model under cyclic weather patterns and varying wind velocities in dryland conditions would provide valuable information about its practical reliability.

Overall, expanding the study to encompass a broader range of dryland scenarios and addressing the in situ challenges faced in actual deserts would contribute to a more comprehensive understanding of material degradation in these regions.

5. Conclusions

With the proliferation of constructions on dry and degraded lands, it is crucial to consider the conditions and characteristics of the surrounding terrain when designing and maintaining outdoor metal structures due to the potential problems caused by wind erosion. However, these parameters are often overlooked during the design process. To address this issue, this study emphasizes the importance of incorporating information about land circumstances in the design and maintenance of metal structures exposed to outdoor conditions.

By developing a predictive model that considers data from diverse sources, it provides valuable insights into the potential degradation and erosion experienced by such structures. The findings underscore the need to include terrain-related parameters as essential factors in the design and maintenance practices for outdoor metal structures.

A comprehensive database was compiled from the existing literature and supplemented with experimental data collected for this study. The tests evaluated the mass loss experienced by metal plates subjected to high-pressure air and sand impacts using direct impingement tests. Sample plates exhibited mass losses ranging from 0.20% to 0.99%. Notably, some plates, such as aluminium and different types of tinplate, showed mass gains, likely due to minimal wear and sand particle embedding.

Based on the literature review and experimental data, a predictive model was developed using the multivariate adaptive regression splines (MARS) algorithm. This model accurately predicted material mass loss based on parameters such as hardness, impact angle, impact velocity, and sand quantity. The practical application of the MARS model was demonstrated in assessing the material performance and durability under different impact conditions, aiding in informed decision-making for product development and material selection. For a relative error of less than 15%, the model shows an efficiency of 98% accuracy.

Future research should focus on studying the influence of wind speed and its parameterization in this context, further enhancing our understanding of material degradation, and enabling more precise modelling and predictions.

Author Contributions: Conceptualization, M.T.-C. and F.O.-F.; methodology, M.D.-P.; validation, V.R.M. and J.V.Á.C.; writing—original draft preparation, M.D.-P. and M.T.-C.; writing—review and editing, M.T.-C. and F.O.-F. All authors have read and agreed to the published version of the manuscript.

Funding: This research was funded by the Council of Science, Innovation, and University through FICYT for the realization of R + D + i network projects with grant number AYUD/2021/57418. Additionally, The APC was funded by the Council of Science, Innovation, and University of the Principality of Asturias with grant number AYUD/2021/50953.

Data Availability Statement: The data used to support the findings of this study are available from the corresponding author upon request.

Conflicts of Interest: The authors declare no conflict of interest.

References

- Wei, X.; Wu, X.; Wang, D.; Wu, T.; Li, R.; Hu, G.; Zou, D.; Bai, K.; Ma, X.; Liu, Y.; et al. Spatiotemporal variations and driving factors for potential wind erosion on the Mongolian Plateau. *Sci. Total. Environ.* **2023**, *862*, 160829. [[CrossRef](#)] [[PubMed](#)]
- Zobeck, T.M.; Van Pelt, R.S.; Hatfield, J.L.; Sauer, T.J. Wind Erosion. In *Soil Management: Building a Stable Base for Agriculture*; John Wiley & Sons, Ltd.: Hoboken, NJ, USA, 2015; pp. 209–227. [[CrossRef](#)]
- Webb, N.P.; Kachergis, E.; Miller, S.W.; McCord, S.E.; Bestelmeyer, B.T.; Brown, J.R.; Chappell, A.; Edwards, B.L.; Herrick, J.E.; Karl, J.W.; et al. Indicators and benchmarks for wind erosion monitoring, assessment and management. *Ecol. Indic.* **2020**, *110*, 105881. [[CrossRef](#)]
- Jarrah, M.; Mayel, S.; Tatarko, J.; Funk, R.; Kuka, K. A review of wind erosion models: Data requirements, processes, and validity. *Catena* **2020**, *187*, 104388. [[CrossRef](#)]
- Woodruff, N.P.; Siddoway, F.H. A Wind Erosion Equation. *Soil Sci. Soc. Am. J.* **1965**, *29*, 602–608. [[CrossRef](#)]
- Williams, J.R.; Jones, C.A.; Dyke, P.T. A Modeling Approach to Determining the Relationship between Erosion and Soil Productivity. *Am. Soc. Agric. Biol. Eng.* **1984**, *27*, 0129–0144. [[CrossRef](#)]
- Liu, B.; Qu, J.; Ning, D.; Han, Q.; Yin, D.; Du, P. WECON: A model to estimate wind erosion from disturbed surfaces. *Catena* **2019**, *172*, 266–273. [[CrossRef](#)]
- Böhner, J.; Schäfer, W.; Conrad, O.; Gross, J.; Ringeler, A. The WEELS model: Methods, results and limitations. *Catena* **2003**, *52*, 289–308. [[CrossRef](#)]
- Hong, C.; Chenchen, L.; Xueyong, Z.; Huiru, L.; Liqiang, K.; Bo, L.; Jifeng, L. Wind erosion rate for vegetated soil cover: A prediction model based on surface shear strength. *Catena* **2020**, *187*, 104398. [[CrossRef](#)]
- Xu, Y.; Liu, L.; Zhou, Q.; Wang, X.; Tan, M.Y.; Huang, Y. An Overview of Major Experimental Methods and Apparatus for Measuring and Investigating Erosion-Corrosion of Ferrous-Based Steels. *Metals* **2020**, *10*, 180. [[CrossRef](#)]
- Savill, T.; Jewell, E.; Barker, P. Development of Techniques and Non-Destructive Methods for In-Situ Performance Monitoring of Organically Coated Pre-Finished Cladding Used in the Construction Sector. In *Electrochemical Society Meeting Abstracts*; The Electrochemical Society, Inc.: Pennington, NJ, USA, 2022; p. 1016. [[CrossRef](#)]
- Laukkanen, A.; Lindgren, M.; Andersson, T.; Pinomaa, T.; Lindroos, M. Development and validation of coupled erosion-corrosion model for wear resistant steels in environments with varying pH. *Tribol. Int.* **2020**, *151*, 106534. [[CrossRef](#)]
- Terrados-Cristos, M.; Ortega-Fernández, F.; Alonso-Iglesias, G.; Diaz-Piloneta, M.; Fernández-Iglesias, A. Corrosion Prediction of Weathered Galvanised Structures Using Machine Learning Techniques. *Materials* **2021**, *14*, 3906. [[CrossRef](#)] [[PubMed](#)]
- Zhang, Y.; Ayyub, B.M.; Fung, J.F. Projections of corrosion and deterioration of infrastructure in United States coasts under a changing climate. *Resilient Cities Struct.* **2022**, *1*, 98–109. [[CrossRef](#)]
- Kok, J.F.; Parteli, E.J.R.; Michaels, T.I.; Karam, D.B. The physics of wind-blown sand and dust. *Rep. Prog. Phys.* **2012**, *75*, 106901. [[CrossRef](#)] [[PubMed](#)]
- Raffaele, L.; Bruno, L. Windblown sand action on civil structures: Definition and probabilistic modelling. *Eng. Struct.* **2019**, *178*, 88–101. [[CrossRef](#)]
- Shao, Y. (Ed.) Integrated Wind-Erosion Modelling. In *Physics and Modelling of Wind Erosion, in Atmospheric and Oceanographic Sciences Library*; Springer: Dordrecht, The Netherlands, 2008; pp. 303–360. [[CrossRef](#)]
- Wang, W.; Samat, A.; Ge, Y.; Ma, L.; Tuheti, A.; Zou, S.; Abuduwaili, J. Quantitative Soil Wind Erosion Potential Mapping for Central Asia Using the Google Earth Engine Platform. *Remote. Sens.* **2020**, *12*, 3430. [[CrossRef](#)]
- Al-Sayed, A.; Al-Shammari, F.; Alshutayri, A.; Aljojo, N.; Aldahri, E.; Abouola, O. The Smart City-Line in Saudi Arabia: Issue and Challenges. *Postmod. Openings* **2022**, *13*, 15–37. [[CrossRef](#)]
- Hunold, C.; Leitner, S. 'Hasta la vista, baby!' The Solar Grand Plan, environmentalism, and social constructions of the Mojave Desert. *Environ. Polit.* **2011**, *20*, 687–704. [[CrossRef](#)]

21. Vo, T.T.E.; Je, S.-M.; Jung, S.-H.; Choi, J.; Huh, J.-H.; Ko, H.-J. Review of Photovoltaic Power and Aquaculture in Desert. *Energies* **2022**, *15*, 3288. [[CrossRef](#)]
22. Parteli, E.J.R. Predicted expansion of sand deserts. *Nat. Clim. Chang.* **2022**, *12*, 967–968. [[CrossRef](#)]
23. Wiesinger, F.; Sutter, F.; Fernández-García, A.; Wette, J.; Wolfertstetter, F.; Hanrieder, N.; Schmücker, M.; Pitz-Paal, R. Sandstorm erosion on solar reflectors: Highly realistic modeling of artificial aging tests based on advanced site assessment. *Appl. Energy* **2020**, *268*, 114925. [[CrossRef](#)]
24. Dentoni, V.; Grosso, B.; Pinna, F.; Lai, A.; Bouarour, O. Emission of Fine Dust from Open Storage of Industrial Materials Exposed to Wind Erosion. *Atmosphere* **2022**, *13*, 320. [[CrossRef](#)]
25. Shi, X. Numerical prediction on erosion damage caused by wind-blown sand movement. *Eur. J. Environ. Civ. Eng.* **2014**, *18*, 550–566. [[CrossRef](#)]
26. El-Sherbiny, Y.M. Erosive wear of different facade finishing materials. *HBRC J.* **2018**, *14*, 431–437. [[CrossRef](#)]
27. Carrascal, I.; Casado, J.; Diego, S.; Polanco, J. Dynamic behaviour of high-speed rail fastenings in the presence of desert sand. *Constr. Build. Mater.* **2016**, *117*, 220–228. [[CrossRef](#)]
28. Hao, Y.-H.; Li, Y. Erosion-behaviors of the coating on steel structure eroded at low erosion-angle in sandstorm. *Mocaxue Xuebao/Tribology* **2013**, *33*, 343–348. [[CrossRef](#)]
29. Hao, Y.-H.; Ren, Y.; Duan, G.-L.; Zhu, M.-X.; Feng, Y.-J. Erosion mechanism and evaluation of steel structure coating eroded under sandstorm environment. *Jianzhu Cailiao Xuebao/J. Build. Mater.* **2014**, *34*, 357–363. [[CrossRef](#)]
30. Cao, X.; He, W.; Liao, B.; Zhou, H.; Zhang, H.; Tan, C.; Yang, Z. Sand particle erosion resistance of the multilayer gradient TiN/Ti coatings on Ti6Al4V alloy. *Surf. Coat. Technol.* **2018**, *365*, 214–221. [[CrossRef](#)]
31. Dalili, N.; Edrissy, A.; Carriveau, R. A review of surface engineering issues critical to wind turbine performance. *Renew. Sustain. Energy Rev.* **2009**, *13*, 428–438. [[CrossRef](#)]
32. Coelho, L.B.; Zhang, D.; Van Ingelgem, Y.; Steckelmacher, D.; Nowé, A.; Terryn, H. Reviewing machine learning of corrosion prediction in a data-oriented perspective. *Npj Mater. Degrad.* **2022**, *6*, 8. [[CrossRef](#)]
33. Bruno, L.; Horvat, M.; Raffaele, L. Windblown sand along railway infrastructures: A review of challenges and mitigation measures. *J. Wind. Eng. Ind. Aerodyn.* **2018**, *177*, 340–365. [[CrossRef](#)]
34. Almajed, A.; Lemboye, K.; Arab, M.G.; Alnuaim, A. Mitigating wind erosion of sand using biopolymer-assisted EICP technique. *Soils Found.* **2020**, *60*, 356–371. [[CrossRef](#)]
35. Meng, H.; Gao, Y.; He, J.; Qi, Y.; Hang, L. Microbially induced carbonate precipitation for wind erosion control of desert soil: Field-scale tests. *Geoderma* **2020**, *383*, 114723. [[CrossRef](#)]
36. Shi, Y.; Shi, Z. Ultrasonic surface treatment for improving wind-blown sand erosion resistance of cementitious materials. *Wear* **2020**, *460–461*, 203185. [[CrossRef](#)]
37. Khanouki, H.A. Development of Erosion Equations for Solid Particle and Liquid Droplet Impact. Ph.D. Thesis, University of Tulsa, Tulsa, OK, USA, 2015.
38. Bouledroua, O.; Meliani, M.H.; Azari, Z.; Sorour, A.; Merah, N.; Pluvinage, G. Effect of Sandblasting on Tensile Properties, Hardness and Fracture Resistance of a Line Pipe Steel Used in Algeria for Oil Transport. *J. Fail. Anal. Prev.* **2017**, *17*, 890–904. [[CrossRef](#)]
39. Pastore, G.; Baird, T.; Vermeesch, P.; Bristow, C.; Resentini, A.; Garzanti, E. Provenance and recycling of Sahara Desert sand. *Earth-Sci. Rev.* **2021**, *216*, 103606. [[CrossRef](#)]
40. Zheng, X.; Bo, T. Representation model of wind velocity fluctuations and saltation transport in aeolian sand flow. *J. Wind. Eng. Ind. Aerodyn.* **2022**, *220*, 104846. [[CrossRef](#)]
41. Oka, Y.; Okamura, K.; Yoshida, T. Practical estimation of erosion damage caused by solid particle impact: Part 1: Effects of impact parameters on a predictive equation. *Wear* **2005**, *259*, 95–101. [[CrossRef](#)]
42. Arabnejad, H.; Mansouri, A.; Shirazi, S.; McLaury, B. *Evaluation of Solid Particle Erosion Equations and Models for Oil and Gas Industry Applications*; SPE: San Antonio, TX, USA, 2015. [[CrossRef](#)]
43. Wiesinger, F.; Sutter, F.; Wolfertstetter, F.; Hanrieder, N.; Fernández-García, A.; Pitz-Paal, R.; Schmücker, M. Assessment of the erosion risk of sandstorms on solar energy technology at two sites in Morocco. *Sol. Energy* **2018**, *162*, 217–228. [[CrossRef](#)]
44. Harsha, A.; Bhaskar, D.K. Solid particle erosion behaviour of ferrous and non-ferrous materials and correlation of erosion data with erosion models. *Mater. Des.* **2008**, *29*, 1745–1754. [[CrossRef](#)]
45. Bingley, M.; O'flynn, D. Examination and comparison of various erosive wear models. *Wear* **2005**, *258*, 511–525. [[CrossRef](#)]
46. Huttunen-Saarivirta, E.; Kinnunen, H.; Tuiremo, J.; Uusitalo, M.; Antonov, M. Erosive wear of boiler steels by sand and ash. *Wear* **2014**, *317*, 213–224. [[CrossRef](#)]
47. Çelik, S.B.; Çobanoğlu, I.; Koralay, T.; Gireson, K. Investigation of the Leeb hardness test in rapid characterisation of rock cores with particular emphasis on the effect of length to diameter ratio. *Int. J. Min. Reclam. Environ.* **2023**, *37*, 524–543. [[CrossRef](#)]
48. ASTM A956/A956m-17a; Standard Test Method for Leeb Hardness Testing of Steel Products. ASTM: West Conshohocken, PA, USA, 2022.
49. ISO 16859-1/2/3:2015; Metallic Materials—Leeb Hardness Test. ISO: Geneva, Switzerland, 2015.
50. ASTM G76-2013; Standard Test Method for Conducting Erosion Tests by Solid Particle Impingement Using Gas Jets. ASTM: West Conshohocken, PA, USA, 2013.
51. Friedman, J.H. Multivariate Adaptive Regression Splines. *Ann. Stat.* **1991**, *19*, 1–67. [[CrossRef](#)]

52. Naser, A.H.; Badr, A.H.; Henedy, S.N.; Ostrowski, K.A.; Imran, H. Application of Multivariate Adaptive Regression Splines (MARS) approach in prediction of compressive strength of eco-friendly concrete. *Case Stud. Constr. Mater.* **2022**, *17*, e01262. [[CrossRef](#)]
53. Praveen, A.S.; Sarangan, J.; Suresh, S.; Subramanian, J.S. Erosion wear behaviour of plasma sprayed NiCrSiB/Al₂O₃ composite coating. *Int. J. Refract. Met. Hard Mater.* **2015**, *52*, 209–218. [[CrossRef](#)]
54. Mathapati, M.; Ramesh, M.; Doddamani, M. High temperature erosion behavior of plasma sprayed NiCrAlY/WC-Co/cenosphere coating. *Surf. Coat. Technol.* **2017**, *325*, 98–106. [[CrossRef](#)]

Disclaimer/Publisher's Note: The statements, opinions and data contained in all publications are solely those of the individual author(s) and contributor(s) and not of MDPI and/or the editor(s). MDPI and/or the editor(s) disclaim responsibility for any injury to people or property resulting from any ideas, methods, instructions or products referred to in the content.